Effective suppression of fluorescence light in Raman measurements using ultrafast time gated charge coupled device camera

D. V. Martyshkin[a)]
Department of Physics, University of Alabama at Birmingham, 1300 University Boulevard, Birmingham, Alabama 35294-1178

R. C. Ahuja
LaVision GmbH, Anna Vandenhoeck Ring 19, D-37081 Goettingen, Germany

A. Kudriavtsev and S. B. Mirov[b)]
Department of Physics, University of Alabama at Birmingham, 1300 University Boulevard, Birmingham, Alabama 35294-1178

(Received 15 September 2003; accepted 7 December 2003)

A high level of fluorescence background signal rejection was achieved for solid and powder samples by using a combination of simple low-resolution spectrograph and ultrafast gated charge coupled device (CCD) camera. The unique timing characteristics of the CCD camera match exceptionally well to characteristics of a Ti:sapphire oscillator allowing fast gated light detection at a repetition rate of up to 110 MHz, making this approach superior in terms of the duty cycle in comparison with other time-resolved Raman techniques. The achieved temporal resolution was about 150 ps under 785 nm Ti: sapphire laser excitation. At an average excitation power up to 300 mW there was no noticeable sample damage observed. Hence, the demonstrated approach extends the capabilities of Raman spectroscopy regarding the investigation of samples with a short fluorescence lifetime. The combination of a spectrometer and a gated CCD camera allows simultaneous study of spectral and temporal characteristics of emitted light. This capability opens an exciting possibility to build a universal instrument for solving multitask problems in applied laser spectroscopy. © *2004 American Institute of Physics.* [DOI: 10.1063/1.1646743]

I. INTRODUCTION

Raman spectroscopy is a powerful method for the characterization of molecules. It has been used for decades as an analytical tool as well as for the study of physical and chemical properties of various materials. Recent developments in laser and detector technologies allow the overcoming of some limitations of this method and are attracting a lot of attention to this spectroscopy in research and industrial laboratories worldwide. It is proven that Raman spectroscopy could be the number one choice for many scientists and engineers due to the high information content in comparison with many other methods.

As with any spectroscopic technique, Raman spectroscopy has certain drawbacks and limitations. The major disadvantage is a low ($\sim 10^{-30}$ cm^2) cross section of Raman scattering. Thus, the Raman signal is weak compared to the fluorescence background and is hard to detect. There are several common methods dealing with the discrimination of Raman scattering from fluorescence, thermal radiation, and stray light.

The discrimination of the out-of-focus background associated with the fluorescence of fluorophores distributed over the sample volume and stray light is successfully realized in confocal Raman microscopy.[1] However, highly fluorescence samples are still beyond the scope of this method.

Another approach is use of ultraviolet (UV) light for sample excitation.[2,3] For the UV excitation, the Raman shifts are usually smaller than the fluorescence Stokes shift of the excited molecules, permitting effective spectral discrimination of the fluorescence. In addition, the majority of the molecules have electronic transitions in the UV region providing conditions for resonance Raman scattering and enhancing the intensity of the Raman bands up to several orders of magnitude.[2,3] However, the problems associated with the samples degradation and the resonance excitation of the fluorescence makes this method suitable for a relatively narrow class of molecules.

Finally, one could avoid fluorescence excitation by tuning the laser wavelength far away from the electronic transitions to the near-infrared (NIR) region, as it is done in Fourier transformed Raman spectroscopy (FTRS). Since the Raman signal decreases as the wavelength in the fourth power, and some organic samples have a strong fluorescence even in the NIR region, FTRS also provides a relatively poor signal to noise ratio.

Not every project requires the use of a confocal microscope. The utilization of simple spectroscopic systems immediately brings about the problem of rejection of stray light associated with the elastic scattering of laser radiation, autofluorescence of cements and coatings in optical elements, multiple reflections in optical elements and spectrometer, and Raleigh scattering in samples. This problem is especially vi-

[a)]Electronic mail: dmartych@phy.uab.edu
[b)]Electronic mail: mirov@uab.edu

tal for the systems equipped with low-resolution spectrometers. The usual approach to reject a stray light is using a notch filter. However, the elastic scattered light can be effectively suppressed by a notch filter only if it is practically collinear to the optical axis. Otherwise, scattered light can propagate though a notch filter substantially increasing the background. Nevertheless, those photons have a longer optical path than Raman photons and therefore are delayed.

There are two major alternative approaches in minimizing the effects of the background signal. One such suppression approach relating to phase resolution was suggested in Ref. 4, where high frequency (150 MHz) sinusoidally modulated light was used to excite rhodamine B in water. It was demonstrated that phase-resolved Raman spectroscopy exploits the phase difference between the fluorescence and Raman emission sinusoids and is capable of resolving the weak Raman scatter from the intense fluorescence. Another background suppression approach is time resolved detection. It is based on the utilization of pulsed excitation and gated signal detection for Raman scattering discrimination from fluorescence,[5] thermal radiation,[6] and stray light in a time domain. The Raman scattering occurs almost instantaneously with a laser pulse while fluorescence lifetimes are in nanosecond or a longer temporal range for the majority of the molecules. The combination of a picosecond excitation pulse with a subnanosecond signal gating provides an affective rejection of the major part of the broad time domain fluorescence signal. On the other hand, the number of Raman photons collected in one acquisition with a picosecond gate would be extremely small. Therefore, the detection system should have a high duty cycle in order to obtain a reasonable signal to the noise ratio. Time-resolved detection has been attracting a considerable amount of attention for a few decades, however, due to technological limitations it was unrealistic for the rejection of fast fluorescence until recently. A brief review can be found in Ref. 7.

Two different approaches of time-resolved detection have been shown to be effective for obtaining Raman spectra from fluorescent samples. The first method used a Kerr gate with a $\sim$3 ps resolution at 650 Hz repetition rate and allows one to detect light with a spectrometer-charge coupled device (CCD) detector combination.[7,8] The system achieved three orders of magnitude suppression of the background from fluorophore with a lifetime of about 2 ns. This method may have an average power of laser radiation of only a few milliwatts, due to a high peak power (MW), which can induce sample damage and nonlinear processes. The second method used a streak camera and provided a resolution of about 10 ps at up to 2 kHz repetition rate for a fluorophore with a fluorescence lifetime of 4 ns.[9]

Due to recent advances in laser and detector technologies, the duty cycle of the detection system could be improved by several orders of magnitude. The approach we used for the time-resolved detection of Raman scattering is based on a combination of the state-of-the-art intensified/gated CCD camera (LaVision ''PicoStar HR''), ultrafast Ti:sapphire oscillator, and a simple short-focal-length spectrograph. This combination allows achieving 150 ps temporal resolution at 76 MHz repetition rate with the average power of laser radiation increased up to 300 mW without noticeable sample damage. Utilization of this approach provided the effective rejection of the fluorescence and stray light background for clear crystalline samples as well as for heterogeneous (powder-like) samples.

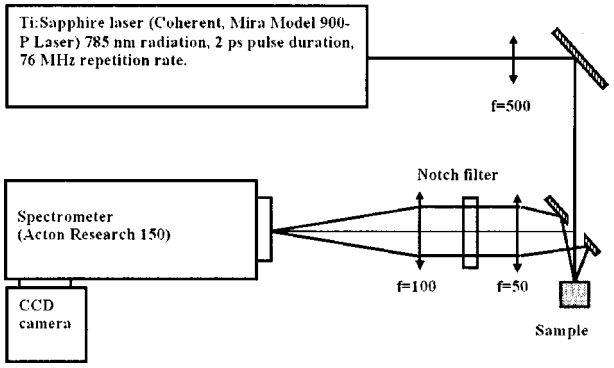

FIG. 1. Raman system optical setup.

II. EXPERIMENT

A. Instrumentation

The optical setup of the Raman system is shown in Fig. 1. The excitation radiation was focused on samples with a long focal length lens to a spot of approximately 400 μm through a 45° mirror. The scattered radiation was collected at 180° with respect to the excitation beam. The super-notch filter (at 785 nm, Kaiser Corp.) was placed inside a two-lens collimator to suppress elastically scattered light. A Ti:sapphire laser (Coherent, Mira model 900-P laser) 785 nm radiation with 2 ps pulse duration at 76 MHz repetition rate was used for excitation. The average power used for the sample excitation was about 300 mW.

The spectrograph-detector combination consists of Acton Research ''SpectroPro-150'' single grating monochromator/spectrograph with a focal length of 150 mm, 1200 g/mm grating, $f/4$ aperture ratio, 16 cm^{-1} resolution, and one of two CCD cameras described later.

The PicoStar HR (LaVision) is a state-of-the-art intensified gated/modulated CCD camera system. The image intensifier is designed for fast gating at a repetition rate up to 110 MHz and a gate width less than 200 ps, jitter less then 20 ps, with photocathode sensitivity in 400–900 nm range. The system equipped with a CCD chip (Interline) 1376×1040 pixels with an ultrafast readout 16 MHz pixel rate at 12 bit (or 10 frames/s) and 65% quantum efficiency.

The second CCD was a conventional thermoelectric cooled TE/CCD camera (Roper Scientific/Princeton Instruments) with a mechanical shutter and 1024×256 pixels CCD chip.

B. Samples

Two highly fluorescent samples have been examined in this study. The crystalline $CaWO_4$ with Nd^{3+} impurities was used as a transparent sample. Hexobenzocoronane (HBC) powder was used as the heterogeneous sample. HBC powder

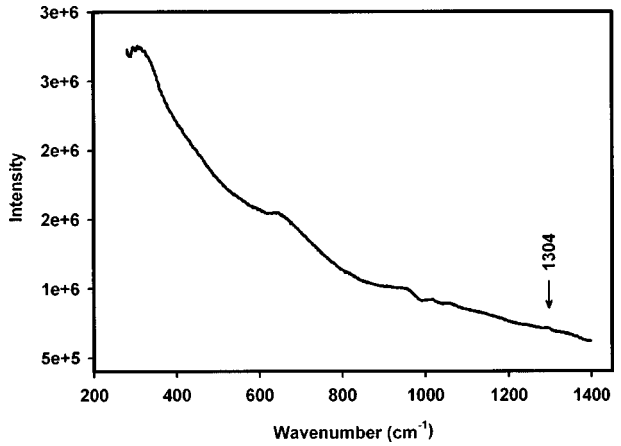

FIG. 2. Raman spectrum of HBC obtained with an ungated CCD camera. The weak band at 1304 cm^{-1} corresponds to HBC Raman scattering. The other bands and strong background are due to a stray light and fluorescence.

was placed in a fused quarts spectroscopic cell. Both samples exhibit a strong fluorescence under 785 nm excitation.

III. RESULTS AND ANALYSIS

A. Rejection of fluorescence

The powder-like samples exhibit a strong elastic scattering of the excitation radiation. The scattered light undergoes diffuse reflection causing a considerable increase of the out-of-focus fluorescence background and a background due to a stray light. Raman spectrum of HBC obtained with an ungated CCD camera is depicted in Fig. 2. The spectrum is an average of 50 acquisitions of 1 s each. HBC is a powder, which has a strong fluorescence even under NIR excitation. As one can see, the background signal overwhelmingly masked a weak Raman scattering signal at 1304 cm^{-1}.

Figures 3(I) and 3(II) demonstrate time resolved light intensity at around 1178 and 1304 cm^{-1} obtained with a gated CCD camera. The spectrum was obtained with a 150 ps gate width and with a 25 ps temporal step between data points. Analysis of Fig. 3 shows that a signal around 1304 cm^{-1} is associated with a combination of HBC Raman bands and fluorescence, while a signal at 1178 cm^{-1} corresponds only to fluorescence. Indeed, Fig. 3(I) shows that two bands have a similar behavior at gate delays longer than 300 ps. Raman scattering could not be detected at such long gate delays and therefore one can see the fluorescence decay only. On the contrary, at short delays, as it is seen in Fig. 3(II), a signal around 1304 cm^{-1} rises faster than the fluorescence signal around 1178 cm^{-1}, indicating the existing additional Raman scattered light in the overall 1304 cm^{-1} signal. The spike at 1200 ps is an artifact due to a stray light, as will be explained later in this article.

The time resolved Raman and the fluorescence spectra of HBC are depicted in Fig. 4. The spectra were obtained with 150 ps gate width at different gate delays. Each spectrum is an average of 50 acquisitions. Raman bands start to appear at 50 ps delay accompanied by a broad fluorescence signal. The most distinct Raman spectra were at 100–150 ps delay. Raman bands diminish completely at 300 ps delay so that one can see the fluorescence only.

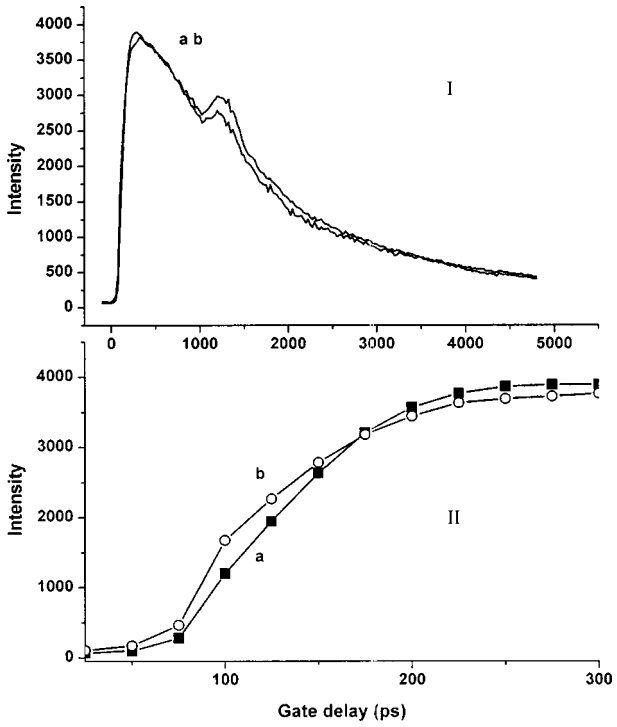

FIG. 3. Time-resolved HBC fluorescence and Raman scattering signal at (a) 1178 and (b) 1304 cm^{-1}. The full-scale signal is shown in (I), while the zoomed initial part of the same kinetics is shown in (II). The signal at (a) 1178 cm^{-1} corresponds to the HBC fluorescence only, while signals at (b) 1304 cm^{-1} are a superposition of the fluorescence and Raman scattering. The signal at 1304 cm^{-1} rises faster than the signal at 1178 cm^{-1} due to additional Raman scattered light. The band at 1200 ps is an artifact due to stray light.

Figure 5 shows the HBC Raman spectrum taken at 100 ps gate delay after broad fluorescence background subtraction. As one can see, we achieved an excellent signal to the background ratio (>100) for a strongly fluorescent powder sample with relatively short fluorescence lifetime.

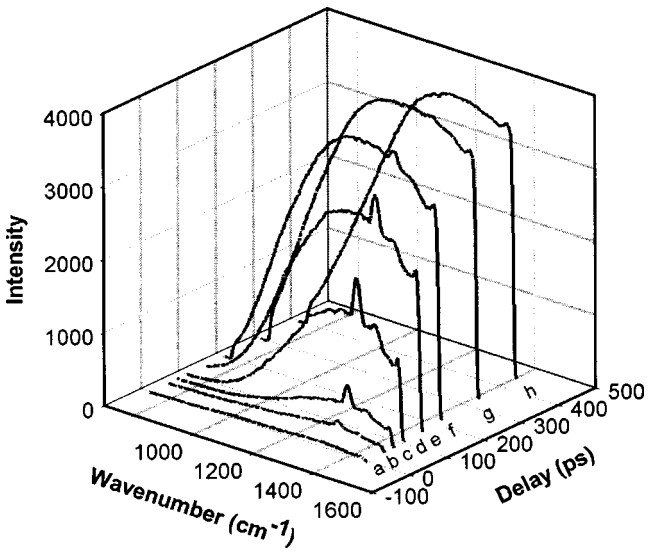

FIG. 4. Time-resolved fluorescence and Raman spectra of the HBC powder. The spectra were taken at (a) 0, (b) 50, (c) 75, (d) 100, (e) 150, (f) 200 ps, (g) 300, and (h) 400 ps gate delay. Each spectrum is an average of 50 acquisitions.

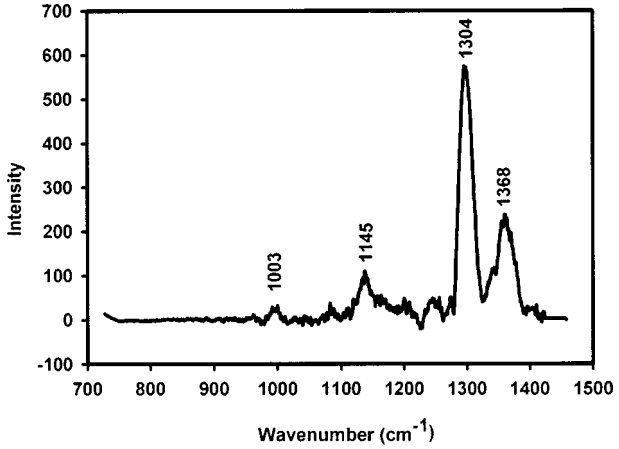

FIG. 5. Stray light and fluorescence rejection from the HBC powder. HBC Raman spectrum is obtained at 100 ps gate delay. The spectrum is an average of 50 acquisitions. The fluorescence background is subtracted.

The study of light emission simultaneously in spectral and temporal domains of the fluorophores with a fluorescence lifetime in nanosecond range is another important capability of the ultrafast time gated detection method. It is particularly important in biomedical spectroscopy, since the majority of endogenous fluorophores have a relatively short lifetime of about 1–5 ns. The data shown previously in Fig. 3 could be used for HBC fluorescence lifetime determination. The data before 2500 ps were contaminated with a stray light, see details in the next section, therefore kinetics after 2500 ps were used for lifetime determination. The linear fit of natural logarithm of the fluorescence intensity is shown in Fig. 6. The time constant was found to be -4.8×10^{8} s^{-1} corresponding to 2.1 ns fluorescence lifetime.

B. Rejection of stray light and luminescence

Figure 7 shows the ungated Raman spectrum of a $CaWO_4$ crystal contaminated with Nd^{3+} ions. The stray light and luminescence background were overwhelming. Only the strongest 912 cm^{-1} Raman band of $CaWO_4$ corresponding to a totally symmetric stretch of vibrations of tetrahedrons

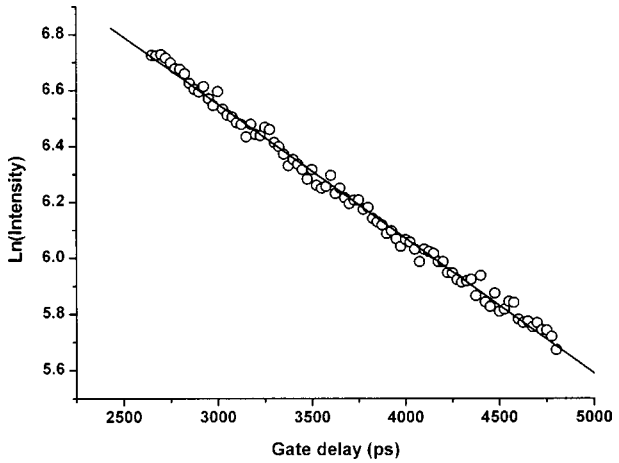

FIG. 6. Linear fit of natural logarithm of the HBC fluorescence intensity. The time constant was found to be -4.8×10^{8} s^{-1} corresponding to 2.1 ns fluorescence lifetime.

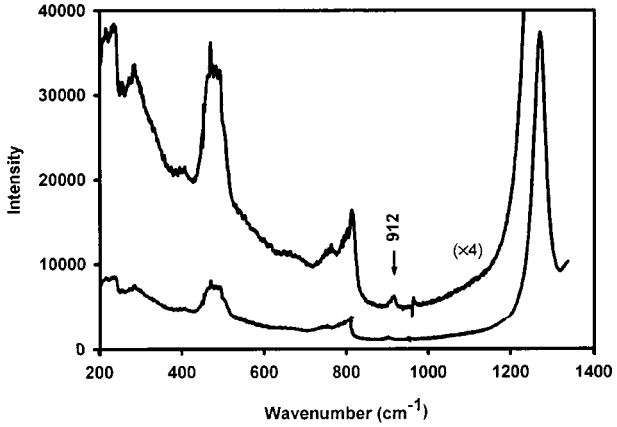

FIG. 7. Raman spectra of the $CaWO_4$ crystal obtained with an ungated CCD camera. The spectrum (a) is an average of 50 acquisitions of 1 s each. Spectrum (b) is the same as (a) multiplied by 4. The 912 cm^{-1} band corresponds to the strongest Raman band of the $CaWO_4$ crystal. The strong 1270 cm^{-1} band corresponds to a fluorescence of Nd^{3+} ($^4F_{3/2}\rightarrow{}^4I_{9/2}$) ions, which are present as an impurity introduced during the crystal growth process. The other bands are due to stray light inhomogeneously distributed over the CCD camera surface.

WO_4^{2-}[10] has been resolved. The strong band at 1270 cm^{-1} (873 nm) was due to the luminescence of Nd^{3+} ($^4F_{3/2}\rightarrow{}^4I_{9/2}$)[11] ions, which were present as an impurity in a $CaWO_4$ crystal. The other bands were due to a stray light inhomogeneously distributed over the CCD surface. The presence of a strong background and artifact bands strongly distort the Raman spectrum and make it impossible to resolve. With a time resolved signal detection, we were able to substantially improve the signal to background ratio by rejecting the stray light and luminescence. Figure 8 shows the total intensity of light that reaches a detector at a different time. The signal was taken by a gated CCD camera in 100 ps temporal intervals and a gate width of about 200 ps. The spectrometer grating was positioned in such a way that Rayleigh scattered excitation radiation can be detected. The signals at 200 and 13 000 ps coincide with laser pulses and

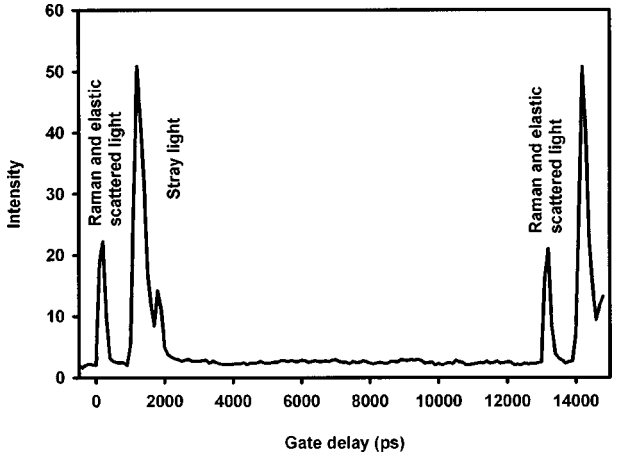

FIG. 8. Time-resolved total light intensity obtained with a gated CCD camera. The temporal step between consequent data points was 100 ps. The gate width was 200 ps. The signals at 200 ps and 13 000 ps coincide with the laser pulses and correspond to the Raman scattered light and elastic scattered light propagating collinear to the optical axis, while strong signals at 1200 and 1800 ps correspond to the overall stray light that reached the CCD camera.

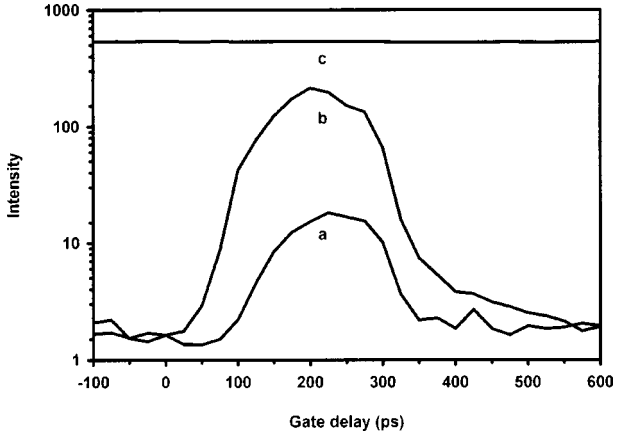

FIG. 9. Time-resolved intensity of Raman bands of the $CaWO_4$ crystal at (a) 797, (b) 912 cm^{-1}, and (c) fluorescence band at 873 nm (1280 cm^{-1}) of Nd impurities in the $CaWO_4$ crystal. The temporal step between consequent data points was 25 ps. The gate width was 200 ps. The temporal FWHM of the Raman band is equal to 200 ps corresponding to the CCD gate width. The fluorescence intensity changes of Nd are not seen, since the fluorescence lifetime is substantially longer than the period of the pump laser oscillations (1 ns).

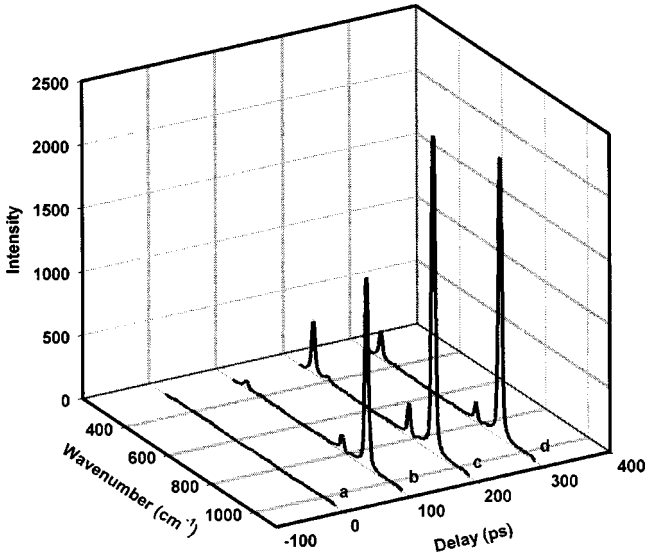

FIG. 10. Time-resolved Raman spectra of the $CaWO_4$ crystal. The spectra were taken at (a) 0, (b) 100, (c) 200, and (d) 300 ps gate delays.

correspond to a combination of Raman and elastically scattered light signals. An elastically scattered light component is due to the Rayleigh scattering that propagates collinearly to the optical axis through the notch filter. Strong signals at 1200 and 14 000 ps correspond to a stray light, which is a superposition of the elastic scattered light in the sample and optical elements of the system, which propagate noncollinearly to the optical axis. It also includes stray light due to multiple reflections on the optical elements and inside the spectrometer. One can see that the stray light is delayed from the Raman signal and could be effectively gated off.

Hence, time-resolved signal detection allows us an effective discrimination of the Raman bands from stray light artifacts and from a luminescence background. The $CaWO_4$ crystal that we used in our study has Nd ions introduced as an impurity during the crystal growth process. The luminescence of rare earth metal ions is usually narrow and could be easily confused with a Raman band if one uses a low-resolution spectrometer. Figure 9 demonstrates time-resolved signals at around 797, 912, and 1280 cm^{-1} (873 nm). The spectrum was taken with 200 ps gate width and with 25 ps temporal step between data points. The 797 and 912 cm^{-1} correspond to the Raman band of the $CaWO_4$ crystal. As one can see, the signal profile has quite a symmetrical shape with a temporal full width at half maximum (FWHM) of about 200 ps, which match the CCD camera gate width. On the contrary, the signal around 1280 cm^{-1} (873 nm) was almost constant. This signal corresponds to the luminescence of Nd^{3+} ($^4F_{3/2} \rightarrow {}^4I_{9/2}$) ions, which a lifetime is considerably longer ($\sim$250 μs) then the time between the laser pulses (1 ns) and therefore the intensity changes of Nd^{3+} luminescence could not be seen in this temporal interval.

The time-resolved Raman spectrum of the $CaWO_4$ crystal obtained with a gated CCD camera is depicted in Fig. 10. The spectrograph grating was positioned in such a way that the Nd impurities luminescence is out of the detection spectral window range. The Raman spectra were acquired at different gate delays. It was strongest at the 200 ps delay, which is in a good agreement with a previous time-resolved intensity profile. Several $CaWO_4$ Raman bands at 335, 405, 797, and 912 cm^{-1} can be clearly resolved with an excellent signal to background ratio. We were able to reconstruct a full $CaWO_4$ Raman spectrum from several spectra obtained at 200 ps gate delay and at different spectrometer grating positions. It is shown in Fig. 11. As one can see, an excellent rejection of stray light and luminescence has been achieved.

Hence, demonstrated time-resolved Raman spectroscopy considerably improve the signal to background ratio and extends the capabilities of Raman measurement regarding the study of samples with short fluorescence lifetime. We have shown that the background from the powder material associated with a stray light and fluorescence can be substantially suppressed even for a simple spectroscopic system equipped with a low-resolution spectrograph and gated CCD camera.

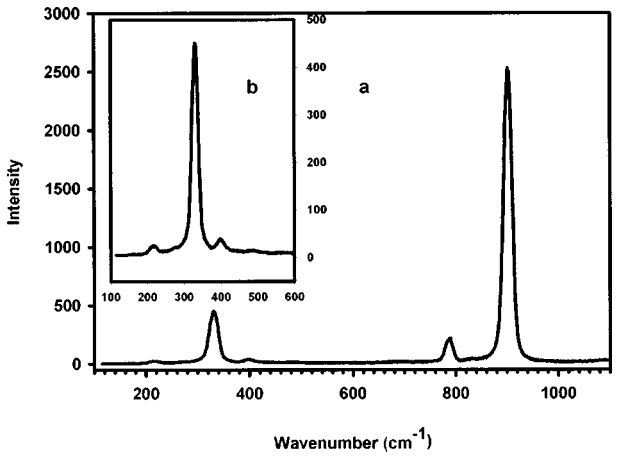

FIG. 11. Stray light and fluorescence rejection from the $CaWO_4$ crystal by a time-resolved light detection. The spectrum (a) was combined from several spectra at different spectrograph grating positions. Spectrum (b) is expanded spectrum (a) in the 100–600 cm^{-1} spectral region.

The high duty cycle (repetition rate 76 MHz) makes this technique superior in comparison to other time-resolved Raman methods.

The study of light emission from a variety of materials simultaneously in spectral and temporal domains opens an exciting opportunity to build a universal instrument. The combination of a gated CCD camera with a confocal microscope will allow performing Raman, resonance Raman, conventional, and time-resolved fluorescence imaging. That kind of robust and easy to operate instrument may have extensive applications in many academic and industrial laboratories.

[1] F. Adar, in *Handbook of Raman Spectroscopy*, edited by I. R. Lewis and H. G. M. Edwards (Marcel Dekker, New York, 2001), pp. 11–40.
[2] M. D. Morris and D. J. Wallam, Anal. Chem. **51**, 182 (1979).
[3] P. R. Carey, *Biochemical Applications of Raman and Resonance Raman Spectroscopies* (Academic, New York, 1982).
[4] F. V. Bright, Anal. Chem. **60**, 1622 (1988).
[5] P. P. Yaney, J. Opt. Soc. Am. **62**, 1297 (1972).
[6] Y. K. Voronko, A. B. Kudryavtsev, A. A. Sobol, and E. V. Sorokin, *Spectroscopy of Oxides Crystals for Quantum Electronics* (Nauka, Moscow, 1991), pp. 50–100.
[7] N. Everall, T. Hahn, P. Matousek, A. W. Parker, and M. Towrie, Appl. Spectrosc. **55**, 1701 (2001).
[8] P. Matousek, M. Towrite, A. Stanley, and A. W. Parker, Appl. Spectrosc. **53**, 1485 (1999).
[9] T. Tahara and H. Hamaguchi, Appl. Spectrosc. **47**, 391 (1993).
[10] A. F. Banishev, Y. K. Voronko, A. B. Kudryavtsev, V. V. Osiko, and A. A. Sobol, Kristallografiya **27**, 618 (1982).
[11] T. V. Verdeyen, in *Laser Electronics*, Prentice Hall Series in Solid State Physical Electronics, 3rd ed., edited by N. Holonyak, Jr. (Prentice-Hall, Englewood Cliffs, NJ, 1995), p. 360.